ISBN: 978-3-95450-132-8 doi:10.18429/JACoW-IPAC2014-THPRO076

FREQUENCY MAPS ANALYSIS OF TRACKING AND EXPERIMENTAL DATA FOR THE SLS STORAGE RING

P. Zisopoulos, Y. Papaphilippou, F. Antoniou, CERN, Geneva, Switzerland
V. Ziemann, University of Uppsala, Uppsala, Sweden
A. Streun, Paul Scherrer Institute, Villigen, Switzerland

Abstract

Frequency Maps Analysis (FMA) has been widely used in beam dynamics in order to study dynamical aspects of the particles linear and non-linear motion, such as optics functions distortion, coupling, tune-shift and resonances. In this paper, FMA is employed to explore the dynamics of models of the Swiss Light Source (SLS) storage ring and compare them with measured turn by turn (TxT) position data. In particular, a method is proposed for estimating the momentum spread using synchrotron sidebands of the Fourier spectrum of the TxT data.

INTRODUCTION

The SLS is a third generation light source which provides photon beams of high brilliance to 20 beam lines. Due to the requirement of producing ultra low equilibrium emittances, the SLS lattice is prone to non-linearities. In order to study the non-linear dynamics of the SLS ring, FMA [1] is applied on the ideal lattice.

An additional aspect of the FMA, is the ability to measure optics properties from TxT experimental data [2]. In this paper, we focus on the estimation of the momentum spread, σ_δ. In this respect, an analytical relationship of σ_δ and its dependence to synchrotron sidebands is deduced and is applied to the BPM TxT data.

FREQUENCY MAPS ANALYSIS

Laskar's FMA obtains the fundamental frequencies of motion from a set of numerically tracked particles. The tracking program PTC is employed for this purpose, for a total of 1056 turns, for on-momentum and for the off-momentum cases $\delta = \pm 1.5\%$. Numerical Algorithm of Fundamental Frequencies (NAFF) [1] performs a refined Fourier analysis to the obtained trajectories, constructing the frequency map of the system. In addition, a diffusion coefficient can be derived by the change in transverse tunes as computed in two consecutive time spans.

In Fig.1, the left plots represent the on momentum case with magnet fringe fields taken into account by the tracking code, whereas the right plots are obtained with fringe fields switched off. The random resonance lines in the frequency maps are shown with blue lines, systematic resonances with red and the dashed lines are resonances due to skew elements. In the first case, the dynamic aperture is clearly reduced compared to the case with fringe fields off. For particles at horizontal amplitude x=5 mm and above, there is a high diffusion zone for small vertical values. This

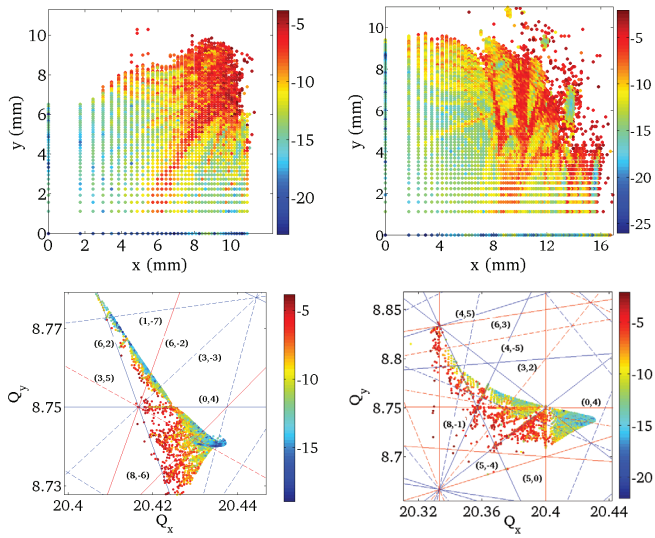

Figure 1: Diffusion (top) and frequency maps (bottom) for the on-momentum case, with (left) and without(right) magnet fringe fields. The color map indicates the frequency diffusion coefficient.

corresponds in the frequency space to the crossing of a multitude of quite high order resonances. There is also Lowering the tune may avoid these resonances. In addition the 4^{th} order resonance seems to cause severe limitations for the particles survival. In the case with no fringe fields, the dynamic aperture is larger as expected although high diffusion zones exist, especially close to the crossing of the 4th and 5th order resonance.

For the off-momentum case, two separate tracking runs were performed for $\delta = \pm 1.5\%$ with fringe fields on and with model chromaticities $Q'_x = 4.92$, $Q'_y = 4.69$, so the working point is expected to move accordingly. Left plots of Fig.2 show the diffusion and frequency map for δ=-1.5%, while right plots show the δ=+1.5% case. For the former case, the dynamic aperture is larger in the vertical plane compared to the on-momentum case with fringe fields on. The main limitation seems to come from the 2nd order sum resonance (1,1) which distorts frequency space and increase diffusion rates for around 6 mm in both planes. For the positive momentum spread, the dynamic aperture is severely limited by the crossing of the 2nd order, half integer horizontal resonance, which limits the horizontal plane at 10 mm and the vertical one at 6 mm.

ISBN: 978-3-95450-132-8 doi:10.18429/JACoW-IPAC2014-THPRO076

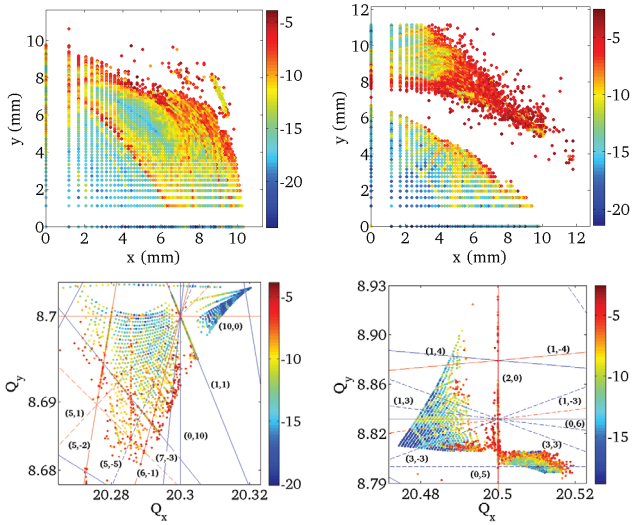

Figure 2: Diffusion (top) and frequency maps (bottom) for off-momentum cases δ=-1.5% (left column) δ=1.5% (right column). The color map indicates the frequency diffusion coefficient.

MOMENTUM SPREAD MEASUREMENTS

The Fourier spectrum of the TxT BPM data in the influence of chromaticity exhibits synchrotron sidebands around the main frequency. The amplitudes A_q of the chromatic sidebands of order q, in the presence of non-linearities, is given by [3]

$$A_q = e^{-s^2}|\bar{a}|\left|I_q(s^2) + \frac{\Delta\beta_1}{4i\beta}\sigma_\delta(is)[I_{q-1}(s^2) - I_{q+1}(s^2)]\right| \quad (1)$$

where $s = \frac{Q'_x\sigma_\delta}{Q_s}$ with Q_s the synchrotron tune and $\bar{a}$ the initial conditions of the beam distribution, $\frac{\Delta\beta_1}{\beta}$ the chromatic beta-beat and I_q the modified Bessel function of the first kind. By using the recursive relationship $I_{q-1}(z) - I_{q+1}(z) = \frac{2q}{z}I_q(z)$, for order q and argument z, Eq.(1) becomes

$$A_q = e^{-s^2}\bar{a}I_q(s^2)(1 + \frac{\Delta\beta_1}{2\beta}\frac{Q_s}{Q'_x}q) \quad (2)$$

This form can be used to derive relationships for σ_δ and $\frac{\Delta\beta_1}{\beta}$. Using Eq.(2) we calculate $\frac{A_1+A_{-1}}{A_0} = \frac{2I_1(s^2)}{I_0(s^2)}$ and the approximation $I_q(z) \approx \frac{1}{\Gamma(q+1)}(\frac{z}{2})^q$ with $\Gamma(q+1) = q!$, can be used. This is only valid if $0 < |z| << \sqrt{q+1}$. For the case of SLS, the theoretical momentum spread is $\sigma_{\delta_{th}} = 8.58 \times 10^{-4}$ and the synchrotron tune is $Q_{s_{th}} = 6.24 \times 10^{-3}$ and $Q'_x = 4.92$, so the condition is met. Using the approximation, we get

$$\sigma_\delta = \pm\frac{Q_s}{Q'_x}\sqrt{\frac{A_1 + A_{-1}}{A_0}} \quad (3)$$

Eq.(3) gives the momentum spread with respect to the Fourier amplitudes of the synchrotron sidebands and the betatron tune. An expression of the chromatic beta-beat can be also obtained as $\frac{\Delta\beta_1}{\beta} = \frac{2Q'_x}{Q_s}\left(\frac{A_1-A_{-1}}{A_1+A_{-1}}\right)$. In the case of symmetric synchrotron sidebands the chromatic beta-beating is zero.

The previous expressions are used to estimate the momentum spread from experimental TxT data. The bunches are kicked transversally to induce coherent oscillations. The period of the bunch centroid is about 200 turns and therefore the synchrotron tune is 5×10^{-3} for the experimental data. Decoherence caused by chromaticity and finite tune spread modulates the bunch centroid's motion and it is damped to zero at half period i.e. 100 turns, while it recoheres at 200 turns. A slow damping is also observed due to synchrotron radiation.

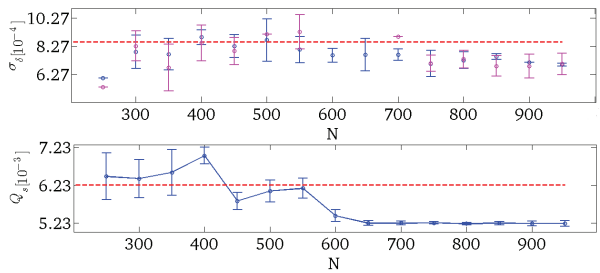

Figure 3: Mean momentum deviation with standard deviation over BPMs vs consecutive turns N for a constant window of 50 turns. Measurements using the positive and negative frequency bands are shown in blue and magenta respectively. The red dashed line indicates the theoretical momentum spread value of SLS. Missing values correspond to failure in synchrotron sidebands measurements.

Amplitudes of the main frequency and its synchrotron sidebands were calculated using NAFF. Using less than 200 turns, synchrotron sidebands were not observed due to resolution of the experimental data. The analysis is done from turn number 200 up to turn number 988, with a constant turn window of 50 turns. The synchrotron tune for each BPM and for every turn window, was computed from the absolute difference between the synchrotron frequencies and the main frequency, for each BPM. The analysis was done for both the positive and the negative harmonics of the frequency spectrum, in order to determine any significant discrepancies. The model value of chromaticity was used. In the top part of Fig. 3, the average measured momentum spread over all BPMs $\langle\sigma_\delta\rangle$ is shown versus the number of turns. In the bottom, the corresponding mean synchrotron tune measurements $\langle Q_s\rangle$ with bars representing one standard deviation is shown, to illustrate the dependence of the synchrotron tune on turns and its effect in momentum spread estimation. From 300 turns to 500 turns, the measurements of momentum spread have an offset of 10^{-5} from the theoretical value with an uncertainty of 10^{-4}. After 500 turns, uncertainty and offset are increased by one order of magnitude. The synchrotron tune

ISBN: 978-3-95450-132-8 doi:10.18429/JACoW-IPAC2014-THPRO076

for the corresponding turns, has an offset of 10^{-4} with uncertainty of 10^{-5} at every turn window except the bump on 400 turns, and after 550 turns, it converges to a value with an offset of 10^{-3} from the theoretical value and zero uncertainty. From already 300 turns, the method is accurate while after 500 turns due to the loss of accuracy in the synchrotron tune measurement, the method is less successful. Between positive and negative frequencies, there were no significant differences observed.

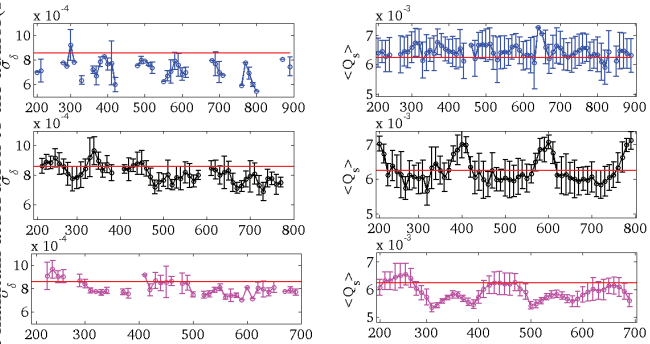

Figure 4: Measured mean momentum spread (left) and synchrotron tune (right) using a sliding window with standard deviation bars with respect to corresponding turns of the measurements. Cases of 100 turns (top blue), 200 turns (middle black) and 300 (bottom magenta) are shown for every 10 measurements for reasons of simplicity. Missing points correspond to failure in measuring synchrotron sidebands at the corresponding turns.

Decoherence and non-linearities induce a turn dependence of beam parameters. In this respect, the second stage of the analysis uses a sliding turn window over consecutive turns, to show the turn dependence of the method. In Fig. 4, average momentum spread and average synchrotron tune measurements over the BPMs vs. their corresponding turn fractions are shown, for three cases, using the positive harmonics. In every case, the synchrotron tune showed an oscillatory behavior with a period depending on the window that was used, while less evident is the oscillation of the momentum spread measurements, the last also showing a slow damping due to the amplitude damping mechanism. Both measurements for the 100 and 200 turns cases, exhibit a period of 100 and 200 turns respectively, while for 300 turns the two oscillations are mixed, giving an oscillation of 300 turns period and a smaller one of 100 turns period. The offset between theoretical value and measurements for the momentum spread and synchrotron tune varies between 10^{-5} and 10^{-3} for all cases, where the least value occurs at the vicinity of each case's period. The uncertainty for both measurements varies between 10^{-5} and 10^{-3}, getting the least value for the 300 turns case, during the turn intervals between the large oscillation. In the case of 100 turns, small uncertainty is explained by the small number of successful sideband measurements at the BPMs. Turn dependence of the synchrotron tune induces a direct turn dependence in the momentum spread measurement.

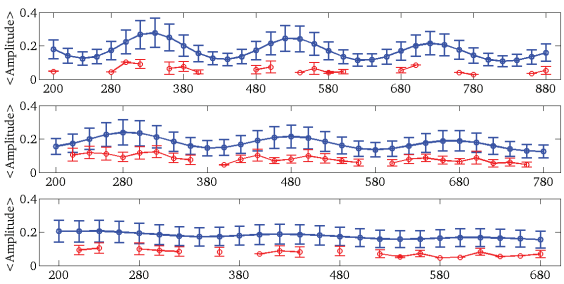

Figure 5: Mean A_0 (in blue) and $A_1 + A_{-1}$ (in red) measurements over the BPMs using a sliding turn window with bars indicating one standard deviation. For reasons of simplicity every 20 measurements are shown. The plots correspond to window widths of 100 turns (top), 200 turns (middle) and 300 turns (bottom). Horizontal axis indicates the corresponding turns for each measurement. Missing points result from failure in measuring synchrotron sidebands at the corresponding turns.

In Fig. 5, the mean $A_1 + A_{-1}$ and A_0 over all BPMs are shown vs their corresponding turns for each window case. For 100 turns, synchrotron sidebands could be only measured between consecutive maxima and minima of A_0. The case of 200 turns provides more data points which explains larger number of successful momentum spread measurements. In 300 turns case all amplitudes converge to a value. This leads to a less oscillatory momentum spread measurement for this case.

CONCLUSIONS

FMA technique was used on the ideal model of SLS, investigating the non-linear dynamics for the on and off-momentum case and revealing dangerous resonances for beam stability. In addition, a method that derives the momentum spread from the synchrotron sidebands of the centroid's motion was tested on experimental TxT data of the SLS. The strong turn dependence of the method induced by decoherence was shown, as well as turn fractions for which the method gives accurate results. The compromise between turn dependent measurements of the synchrotron tune and synchrotron sidebands define the efficiency of the method. This technique is still under development along with the chromatic beta-beat measurements performing an analysis at the same manner.

REFERENCES

[1] J. Laskar, "Frequency map analysis and particle accelerators", Proceedings of the 2003 PAC.

[2] P. Zisopoulos, Y. Papaphilippou, A. Streun, V. Ziemann, Beam optics measurements through turn by turn position data in the SLS, IPAC 2013, WEPEA067.

[3] G. Rumolo, F. Schmidt, R. Tomas, Decoherence of a longitudinally kicked beam with chromaticity, NIMA A528 (2004) 670-676.